HYPERSONIC HEAT-TRANSFER AND TRANSITION CORRELATIONS FOR A ROUGHENED SHUTTLE ORBITER

John J. Bertin, Dennis D. Stalmach, Ed S. Idar and Dennis B. Conley
The University of Texas at Austin

Winston D. Goodrich
Johnson Space Center

SUMMARY

The effect of roughness on the heat-transfer distributions and the transition criteria for the windward pitch plane of the Shuttle Orbiter at an angle of attack of 30° was studied using data obtained in hypersonic wind tunnels. The heat-transfer distributions and the transition locations for the roughened models were compared with the corresponding data for smooth models. The data were correlated using theoretical solutions for a nonsimilar, laminar boundary layer subject to two different flow-field models for the Orbiter.

INTRODUCTION

In order to predict the convective heat-transfer distribution for the windward surface of the Space Shuttle entry configuration, one must develop engineering correlations for the three-dimensional, compressible boundary layer. Since the aerodynamic heating rates generated by a turbulent boundary layer may be several times greater than those for a laminar boundary layer at the same flight condition, the correlations must include a transition criteria suitable for the complex flow fields. Because the windward surface of the Orbiter is composed of a large number of thermal protection tiles, the transition criteria must include the effect of the distributed roughness arising from the joints and possible tile misalignment. Thus, the transition correlation is complicated by the presence of roughness which interacts with other transition-related parameters. As discussed in reference 1, parameters, such as wall cooling, which decreases the boundary-layer thickness and delays transition on a smooth body, might actually promote transition for a given surface roughness. Morrisette (ref. 2) found that although the effective roughness Reynolds number increases significantly in the presence of a favorable pressure gradient near the centerline, much smaller roughness was required to promote transition near the shoulder of an Orbiter configuration, where again there was a favorable pressure gradient (this one associated with cross flow).

During tests in which a ring of spherical roughness elements were located in a supersonic flow past a cone, Van Driest and Blumer (ref. 3) observed variations in the relative roles played by the disturbances in the basic flow field

and those resulting from the presence of roughness elements. For some conditions, the disturbances associated with the basic flow field were predominant in establishing transition, whereas for other flows, the roughness elements dominated the transition process.

McCauley et al (ref. 4) found that the spherical roughness elements required to trip the boundary layer on sphere noses were several times larger than the boundary-layer thickness, whereas the trips required for a cone were within the boundary layer. Heat-transfer data (ref. 5) obtained in Tunnel B of the Arnold Engineering Development Center (AEDC) for a 0.04-scale Orbiter indicated that a ring of spherical trips, which were 0.079 cm. (0.031 in.) in diameter and were 0.11L from the nose, caused the transition location to move considerably upstream of the natural transition location (i.e., that for a smooth body). In the same test program (ref. 5), a simulated interface gap between two insulation materials, which was 0.102 cm. (0.040 in.) wide by 0.203 cm. (0.080 in.) deep and was located at x = 0.02L, had no measurable effect on boundary-layer transition at $\alpha = 40°$ and $Re_{\infty,L} = 8.6 \times 10^6$. In a series of tests using delta-wing Orbiter models (ref. 6), premature boundary-layer transition was observed on a model having simulated heat-shield panels with raised joints. Slot joints, however, did not cause premature transition of the boundary layer. The former model featured a series of transverse panels 0.635 cm. (0.250 in.) wide separated by a raised retaining strip 0.025 cm. (0.010 in.) wide by 0.0025 cm. (0.001 in.) high. The panels on the model with slotted joints were 0.635 cm. (0.250 in.) square separated by slots 0.020 cm. (0.008 in.) wide by 0.005 cm. (0.002 in.) deep. The Reynolds number ($Re_{\infty,L}$) for these tests ranged from 6.5×10^6 to 9.0×10^6 using a model 0.403 m (1.321 ft.) long.

The present paper discusses the results of an experimental investigation in which heat-transfer data were obtained on a Shuttle Orbiter model for which the first 80% of the windward surface was roughened either by a simulated vertical tile misalignment or by a grit-blasting technique. The misaligned tiles were 0.0023 cm. to 0.0025 cm. high on the 0.0175-scale Orbiter. Heat-transfer data were obtained in Tunnel B and in Tunnel F over a Mach number range from 8.0 to 12.1 and over a Reynolds number range (based on model length) from 1.17×10^6 to 17.63×10^6.

SYMBOLS

h	local heat-transfer coefficient, $\dot{q}/(T_t-T_w)$
$h_{t,ref}$	heat-transfer coefficient for the reference stagnation-point heating rate
k	height of roughness element
L	axial model length, 0.574 m (1.882 ft)
msf	metric scale factor equal to the equivalent radius divided by L

M_e local Mach number at the edge of the boundary layer

M_∞ free-stream Mach number

r_{ref} radius of reference sphere reduced to model scale, 0.5334 cm. (0.0175 ft.)

Re_{ns} Reynolds number behind a normal shock, $\rho_{ns} u_{ns} r_{ref} / \mu_{ns}$

Re_s Reynolds number based on local flow properties integrated over the length from the stagnation point to the point of interest

$Re_{\infty,L}$ free-stream Reynolds number based on model length

Re_θ Reynolds number based on local flow properties at the edge of the boundary layer and on the momentum thickness

x axial coordinate

δ^* displacement thickness

The subscript tr designates parameters evaluated at the transition location.

EXPERIMENTAL PROGRAM

The experimental program was conducted to investigate what effect tile misalignment representative of a reasonable manufacturing tolerance has on heat-transfer and transition criteria in the plane of symmetry of the Shuttle Orbiter. Thus, a 0.0175-scale Orbiter model, which had been tested previously in a smooth surface condition in Tunnel B and in Tunnel F of the AEDC was modified. Selected tiles, slightly raised above the model surface, were precisely deposited on the windward surface using an electroless plating technique (ref. 7). Heat-transfer rates to the tile-roughened model were obtained first in Tunnel B and then in Tunnel F. However, 60% of the tiles were lost from the model during the initial runs of the Tunnel F program. After the initial runs, the remaining tiles were removed and the windward surface roughened by a grit-blasting technique.

Model. - The model used in the test programs (see the sketch of Fig. 1) was a 0.0175-scale model of the 29-0 Shuttle Orbiter. Twenty-seven coaxial surface thermocouples were used to obtain the heat-transfer-rate distribution for the windward plane of symmetry. The uncertainty for most of the heat-transfer-rate measurements was approximately 10% (refs. 8 and 9).

Tile roughness. - A herringbone pattern (symmetric about the plane of symmetry) of raised tiles covered the windward surface of the Orbiter model up to the tangent line of the chines from x = 0.02L to 0.80L. The raised tiles, which were selected randomly, represented 25% of the tiles in the area of interest as shown in the photograph of Fig. 2. The selected tiles were 0.267 cm. (0.105 in.) square and were 0.0023 cm. (0.0009 in.) to 0.0025 cm. (0.0010 in.) in height.

The vertical misalignment, thus simulated, of 0.1306 cm. (0.0514 in.) to 0.1451 cm. (0.0571 in.) full scale was considered representative of manufacturing tolerance.

Grit roughness. - The tiles remaining after the initial runs of the Tunnel F program were removed and the surface roughened over the first 80% of the windward surface using a grit-blasting technique. The average peak-to-valley distance for ten readings in a 0.25 cm. (0.10 in.) length as read from a photomicrograph was 0.0041 cm. (0.0016 in.).

Test Program. - Heat-transfer rates were obtained in Tunnel B at a free-stream Mach number of 8 over a range of Reynolds number (based on model length) from 1.89×10^6 to 7.07×10^6. The surface temperature for the Tunnel B tests varied from 0.40 T_t to 0.43 T_t. For the Tunnel F tests the Mach number varied from 10.73 to 12.06 while the Reynolds number varied from 1.17×10^6 to 17.63×10^6. The surface temperature for the Tunnel F tests varied from 0.14 T_t to 0.28 T_t. The data presented in the present paper were obtained at an angle of attack of 30°.

For additional details regarding the model or the test program, the reader is referred to references 8 and 9.

THEORETICAL SOLUTIONS

Theoretical solutions for a nonsimilar, laminar boundary layer were generated for the pitch plane of the Orbiter model at an angle of attack of 30° to determine the flow properties at the transition location. The theoretical solutions were computed using a modified version of the code described in reference 10. Required as input for the code are the flow conditions at the edge of the boundary layer, the radius of the "equivalent" body of revolution, and the wall-temperature distribution. The metric scale-factor describing the streamline divergence was used to represent the radius of the equivalent body of revolution in the axisymmetric analogue for a three-dimensional boundary layer. The metric coefficients were calculated using the relations described by Rakich and Mateer (ref. 11).

Two different flow-field models were used to generate the required inviscid solution for the plane of symmetry. The pressure distribution and the streamlines for the first flow model, designated "Newt, NSE", represent modified Newtonian flow. For this flow model, it was assumed that the fluid at the edge of the boundary layer was that which had passed through the normal portion of the bow shock wave and had accelerated isentropically from the stagnation point. The inviscid flow properties for the second flow-field model, designated "LFF, VarEnt", were supplied by the Lockheed Electronics Company using the code described in reference 12. This flow model accounts for the entropy variation in the shock layer which results because of the curvature of the shock wave. Thus, the entropy of the fluid at the edge of the boundary layer varied with distance from the apex. The pressure distributions and the metric

scale-factor distributions, thus calculated for a free-stream Mach number of 8 (the nominal value of the Tunnel B tests) and for $\alpha = 30°$, are presented in Figure 3 for the two flow models. Whereas the pressure distributions are similar, significant differences exist in the local entropy distribution and in the metric scale-factor distributions for the two flow models. As a result, the values for local flow properties, such as the velocity, the Mach number, and the unit Reynolds number, were much higher for the LFF, VarEnt model than for the Newt, NSE model.

EXPERIMENTAL DATA FOR AN ANGLE OF ATTACK OF 30°

The heat-transfer measurements for the tile-roughened models are compared in Figure 4 with the heat-transfer data obtained in a previous Tunnel B program (ref. 13) in which a smooth model was subjected to essentially identical flow conditions. The experimental values for the local heat-transfer coefficients have been divided by the theoretical value for the stagnation point of a 0.5334 cm. (0.0175 ft.) radius sphere as calculated using the theory of Fay and Riddell (ref. 14). For purposes of data presentation the recovery factor has been set equal to unity. For $x \leq 0.90L$, the local heat transfer coefficients for the tile-roughened model were typically between 8% to 26% greater than those for the smooth model. This was true both for the laminar and for the transitional portions of the boundary layer. The data for the thermocouple at $x = 0.20L$ were counter to this trend, but the measurements at this thermocouple are believed to be slightly low for the tile-roughened model (refer also to Fig. 5). At the downstream end of the model, i.e., $0.90L < x < 1.00L$, the local heat-transfer coefficients were approximately the same (i.e., within the uncertainty of the measurements) when the boundary layer was transitional or turbulent. There were not sufficient data for fully turbulent boundary layers at comparable flow conditions to warrant general conclusions. For the lowest Reynolds number tests, the heat transfer at the downstream end of the tile-roughened model was from 25% to 55% greater than that of the smooth model. However, since these heating rates were relatively low, the experimental uncertainty of the data was between 10% to 25% (ref. 8). The increased heating, which was significantly greater than the experimental uncertainty, may be due to roughness-induced perturbations to the relatively thick laminar boundary layer or to the slightly premature onset of transition. Since the roughness presented by the vertical misalignment of the tiles perturbed the flow sufficiently to produce weak shock waves (refer to the shadowgraphs presented in ref. 7), the increased heating evident in the data of Figure 4 is not unexpected.

Experimentally determined heat-transfer data obtained in Tunnel B for the tile-roughened model are compared in Figure 5 with the theoretical solutions for a laminar boundary layer. Despite the roughness-induced perturbations to the heat transfer, the experimental laminar values are between the theoretical values for the two flow-field models. The streamwise variation of the measurements more closely follows the theoretical distribution based on the LFF, VarEnt flow model. Thus, the data indicate that one should include the variations in entropy when developing correlations for the aerothermodynamic environment of the Shuttle. The departure of the experimental heat-transfer

measurements from the laminar correlation, which is indicated by the arrows in Figure 5, was defined as the onset of transition.

The experimentally determined heat-transfer distributions obtained in Tunnel F for the tile-roughened model are presented in Figure 6. From $0.20L \leq x < 0.55L$, the heat-transfer measurements for the two higher Reynolds-number flow conditions were as much as 30% above the corresponding values for the lowest Reynolds number. These locally high heating rates may be an indication of "incipient" transition. As will be discussed later, the transition correlation parameter (using local properties based on the LFF, VarEnt flow model) was relatively low for these two flow conditions. Thus, if these data are indeed indicative of "incipient" transition, the favorable pressure gradient inhibited the transition process and the boundary layer was laminar for $x > 0.60L$. Again, the experimentally determined laminar heat-transfer coefficients were in reasonable agreement with the theoretical values calculated using LFF, VarEnt flow model.

Experimentally determined heat-transfer distributions obtained in Tunnel F for the grit-roughened model are presented in Figure 7. For the highest Reynolds-number flow condition (i.e., $Re_{\infty,L} = 13.45 \times 10^6$), transition occurred at $x = 0.06L$. It should be noted that a strong favorable pressure gradient existed in this region (see Fig. 3a). With transition occuring so near the stagnation point, the theoretical value for the boundary-layer displacement thickness was less than the average peak-to-valley distance for the grit roughness (i.e., $\delta_{tr}^* = 0.351\ k$ for Newt, NSE and $\delta_{tr}^* = 0.434\ k$ for LFF, VarEnt). Thus, the grit may have been effective in tripping the boundary layer for the highest Reynolds-number flow. As the Reynolds number decreased, transition moved downstream and the grit-roughness elements became immersed in the boundary layer. Using the theoretical values for the LFF, VarEnt flow model, δ_{tr}^* was 0.684 k, 4.90 k, and 7.67 k when $Re_{\infty,L}$ was 9.45×10^6, 7.51×10^6, and 3.99×10^6, respectively. The heat-transfer measurements for $Re_{\infty,L} = 7.51 \times 10^6$ were slightly greater than the companion laminar measurements from $x = 0.20L$ to the assumed transition location (i.e., $x_{tr} = 0.40L$). Again, the possibility exists that the data indicate a roughness-induced incipient transition process countered by a stabilizing pressure gradient.

Although the local heating was measurably increased by the tile misalignment, the Tunnel B data of Figure 4 indicated that the transition locations were not affected by tile misalignment of the magnitude considered in the present tests. Pate (ref. 15) has found that, to a significant degree, the tripped location at supersonic speeds is dependent on the free-stream disturbances in a tunnel. He concluded that it appeared appropriate to relate roughness effects by comparing the roughened-model transition locations to the smooth-wall transition location when attempting to normalize tunnel flow effects. Therefore, the effect of roughness on the present transition locations is indicated by comparing smooth-wall data with rough-model data from the same tunnel as a function of Re_{ns}. Data obtained in Tunnel B for a smooth model (ref. 13) and for a tile-roughened model (ref. 8) are presented in Figure 8a.

Data obtained in Tunnel F for a smooth model (ref. 16) and for a grit-roughened model (ref. 9) are presented in Figure 8b. It is evident that the roughness elements of the present tests caused premature transition only for the highest Reynolds-number flow conditions in Tunnel F. These were the only flow conditions for which δ_{tr}^* was less than k, the roughness height. It should also be noted that the grit-blasted roughness, which promoted transition in these runs, was greater in height than the misaligned tiles.

Values for the transition correlation parameters, $(Re_\theta/M_e)_{tr}$ and $Re_{s,tr}$, which have been calculated using the two flow-field models, are presented in Figure 9. As noted previously, even though the pressure distributions are similar, the assumed flow process (i.e., an isentropic expansion from the stagnation point or an adiabatic process subject to the entropy distribution defined by the shock shape) had a profound effect on the local flow properties. Note a single value for either transition parameter, i.e., $(Re_\theta/M_e)_{tr}$ or $Re_{s,tr}$, was not found from the correlations made using either flow model. For the Newt, NSE flow model, $(Re_\theta/M_e)_{tr}$ is approximately equal to 0.348 $(Re_{s,tr})^{0.5}$. The correlation for the parameters evaluated based on the LFF, VarEnt flow model is not as simple. The data may be considered as falling into one of three groups: (1) the roughness-promoted transition which occured in the highly favorable pressure gradient near the nose (i.e., the open symbols for $Re_{s,tr} < 400{,}000$), (2) the incipient transition locations for the data discussed in Figure 6 (i.e., the filled symbols), and (3) the remaining data for which the transition locations were unaffected by model roughness (i.e., the open symbols for $Re_{s,tr} > 900{,}000$). These data are being studied further.

CONCLUDING REMARKS

Heat-transfer data for the Shuttle Orbiter at an angle of attack of 30° have been obtained in Tunnel B and in Tunnel F. The first 80% of the windward surface of the model was roughened either by a simulated vertical tile misalignment or by a grit-blasting technique. Based on the data obtained in these tests, the following conclusions are made.

(1) Surface roughness of the magnitude considered did not have a significant effect on the transition location until the Reynolds number was sufficiently high to cause transition near the nose. At these high Reynolds numbers, the roughness elements became large relative to the boundary layer and became effective as tripping elements.

(2) The local heat-transfer coefficients for the tile-roughened model were measurably greater than the corresponding values for the smooth model. This was true both for the laminar and for the transitional portions of the boundary layer.

(3) Both theoretical flow models produced heat-transfer distributions which were in reasonable agreement with the magnitude of the laminar data. The

flow model which included the entropy gradients in the flow field, i.e., the "more exact" LFF, VarEnt flow model, provided a better correlation of the streamwise variation in heating. The two theoretical models produced markedly different correlations for the transition parameters. Additional study is needed to define the impact of these variations on the correlations for flight conditions.

REFERENCES

1. Braslow, A.L., "A Review of Factors Affecting Boundary-Layer Transition", NASA TND-3384, Apr. 1966.

2. Morrisette, E.L., "Roughness Induced Transition Criteria for Space Shuttle-Type Vehicles", Journal of Spacecraft and Rockets, Feb. 1976, Vol. 13, No. 2, pp. 118-120.

3. Van Driest, E.R., and Blumer, C.B., "Boundary-Layer Transition at Supersonic Speeds - Three-Dimensional Roughness Effects (Spheres)", Journal of the Aerospace Sciences, Aug. 1962, Vol. 29, No. 8, pp. 909-916.

4. McCauley, W.D., Saydah, A.R., and Bueche, J.F., "Effect of Spherical Roughness on Hypersonic Boundary-Layer Transition", AIAA Journal, Dec. 1966, Vol. 4, No. 12, pp. 2142-2148.

5. Carver, D.B., "Heat-Transfer Tests on the Rockwell International Space Shuttle Orbiter with Boundary-Layer Trips (OH-54)", AEDC-TR-76-28, May 1976.

6. Seegmiller, H.L., "Effects of Roughness on Heating and Boundary Layer Transition, Part I - Effects of Simulated Panel Joints on Boundary-Layer Transition", Space Shuttle Aerothermodynamics Technology Conference, Volume II-Heating, NASA TM X-2507, February 1972.

7. Stalmach, C.J., Jr., and Goodrich, W.D., "Aeroheating Model Advancements Featuring Electroless Metallic Plating", presented at the AIAA 9th Aerodynamic Testing Conference in Arlington, Texas, June 1976.

8. Siler, L.G., and Martindale, W.R., "Test Results from the NASA Space Shuttle Orbiter Heating Test (MH-2) Conducted in the AEDC-VKF Tunnel B", AEDC-DR-75-103, Oct. 1975.

9. Siler, L.G., "Test Results from the NASA Space Shuttle Orbiter Heating Test (MH-1) Conducted in the AEDC-VKF Tunnel F", AEDC-DR-76-13, Mar. 1976.

10. Bertin, J.J., and Byrd, O.E., Jr., "The Analysis of a Nonsimilar Boundary Layer - A Computer Code (NONSIMBL)", University of Texas at Austin, Aerospace Engineering Report 70002, Aug. 1970.

11. Rakich, J.V., and Mateer, G.G., "Calculation of Metric Coefficients for Streamline Coordinates", AIAA Journal, Nov. 1972, Vol. 10, No. 11, pp. 1538-1540.

12. Goodrich, W.D., Li, C.P., Houston, C.K., Chiu, P., and Olmedo, L., "Numerical Computations of Orbiter Flow Fields and Heating Rates", AIAA Paper 76-359, presented at the AIAA 9th Fluid and Plasma Dynamics Conference, San Diego, Cal., July 1976.

13. Martindale, W.R., and Trimmer, L.L., "Test Results from the NASA/Rockwell International Space Shuttle Test (OH4A) Conducted in the AEDC-VKF Tunnel B", AEDC-DR-74-39, May 1974.

14. Fay, J.A., and Riddell, F.R., "Theory of Stagnation Point Heat Transfer in Dissociated Air", Journal of the Aeronautical Sciences, Feb. 1958, Vol. 25, No. 2, pp. 73-85, 121.

15. Pate, S.R., "Supersonic Boundary-Layer Transition:Effects of Roughness and Freestream Disturbances", AIAA Journal, May 1971, Vol. 9, No. 5, pp. 797-803.

16. Boudreau, A.H., "Test Results from the NASA/RI Shuttle Heating Test OH-11 in the AEDC-VKF Tunnel F", AEDC-DR-74-16, Feb. 1974.

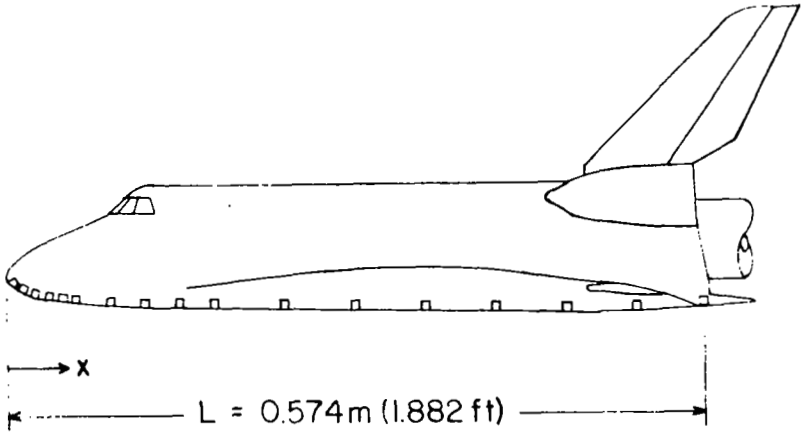

Fig. 1. - Sketch of the 0.0175-scale Orbiter model.

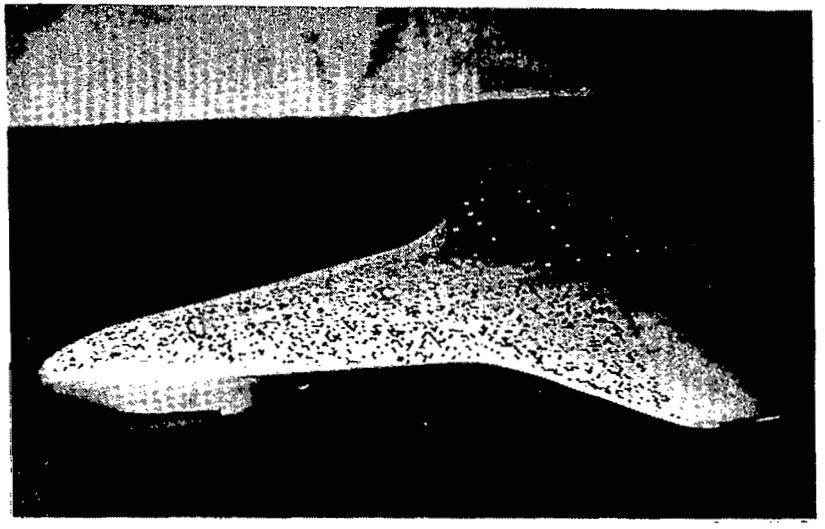

Fig. 2. - Photograph of the Orbiter model showing the vertically misaligned tiles (plated to 0.0023 cm. in height).

Fig. 3. - A comparison of the inviscid flow-field parameters for M_∞ = 8 flow past the Orbiter at α=30°.

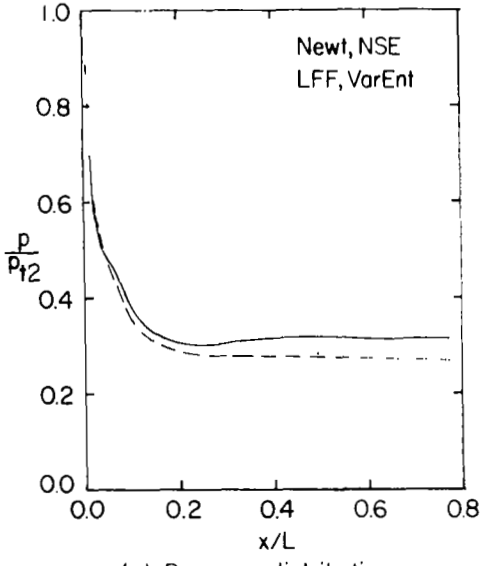

(a) Pressure distribution

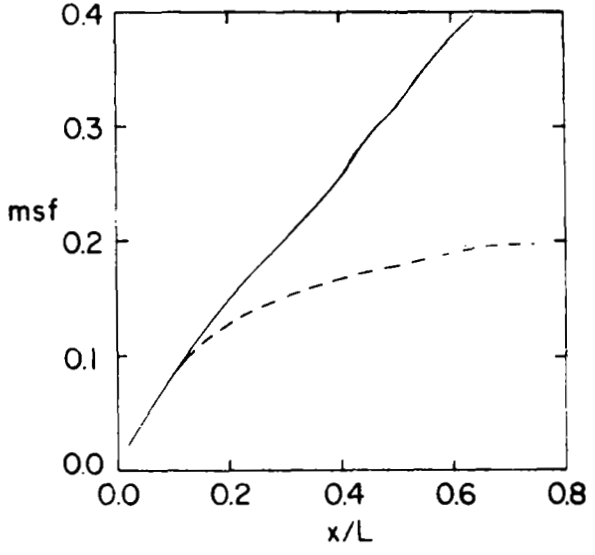

(b) Metric scale-factor distribution

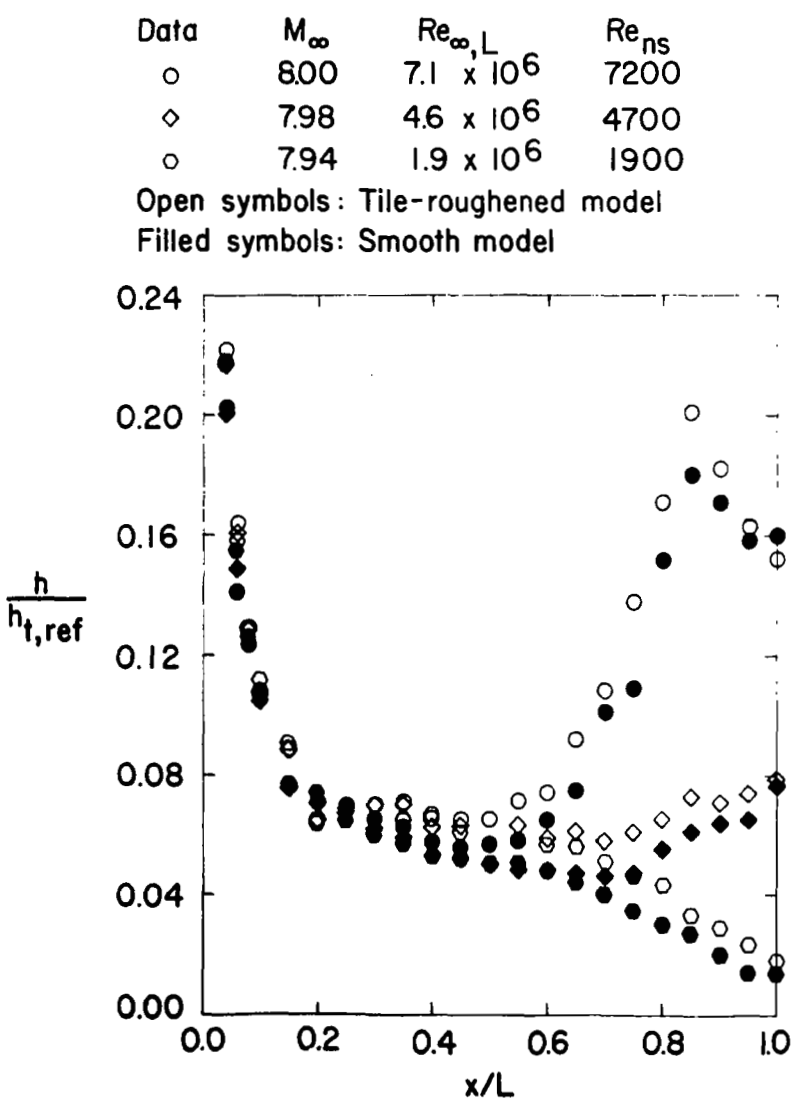

Fig. 4. - The effect of tile roughness on the heat-transfer distributions obtained in Tunnel B for $\alpha = 30°$.

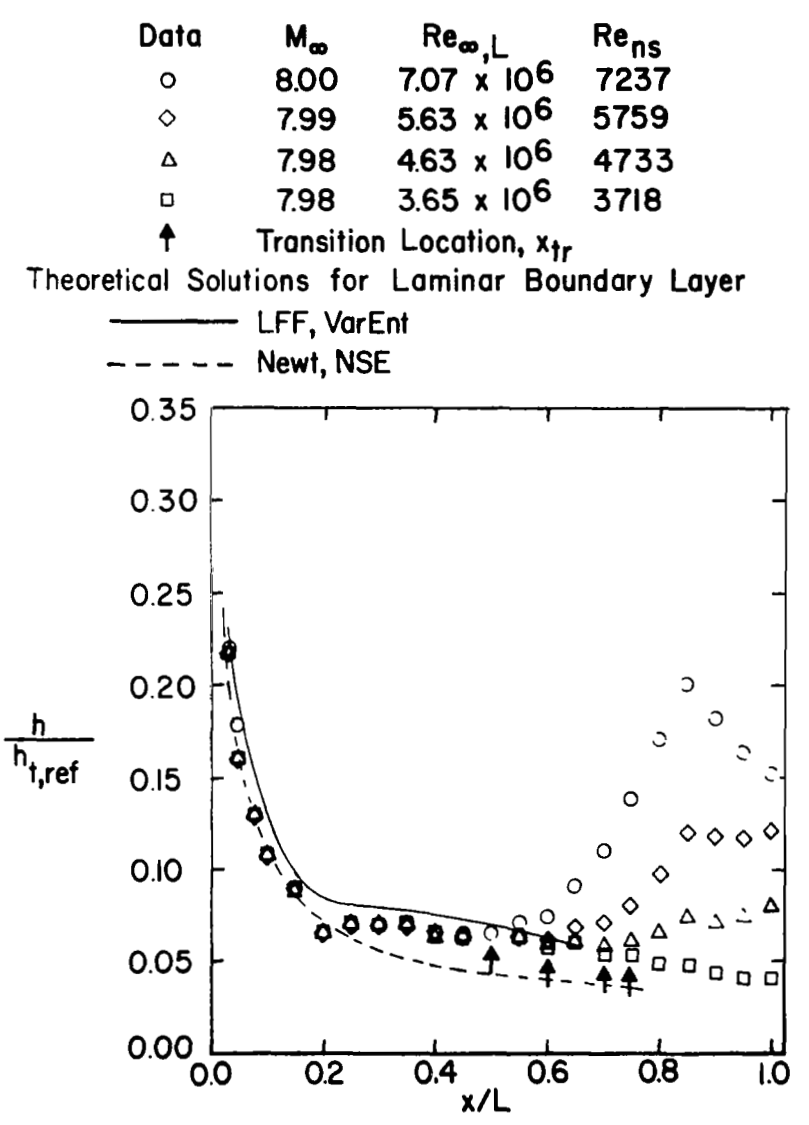

Fig. 5. - Heat-transfer distributions from the plane of symmetry of the tile-roughened model (Tunnel B) compared with theoretical laminar distributions.

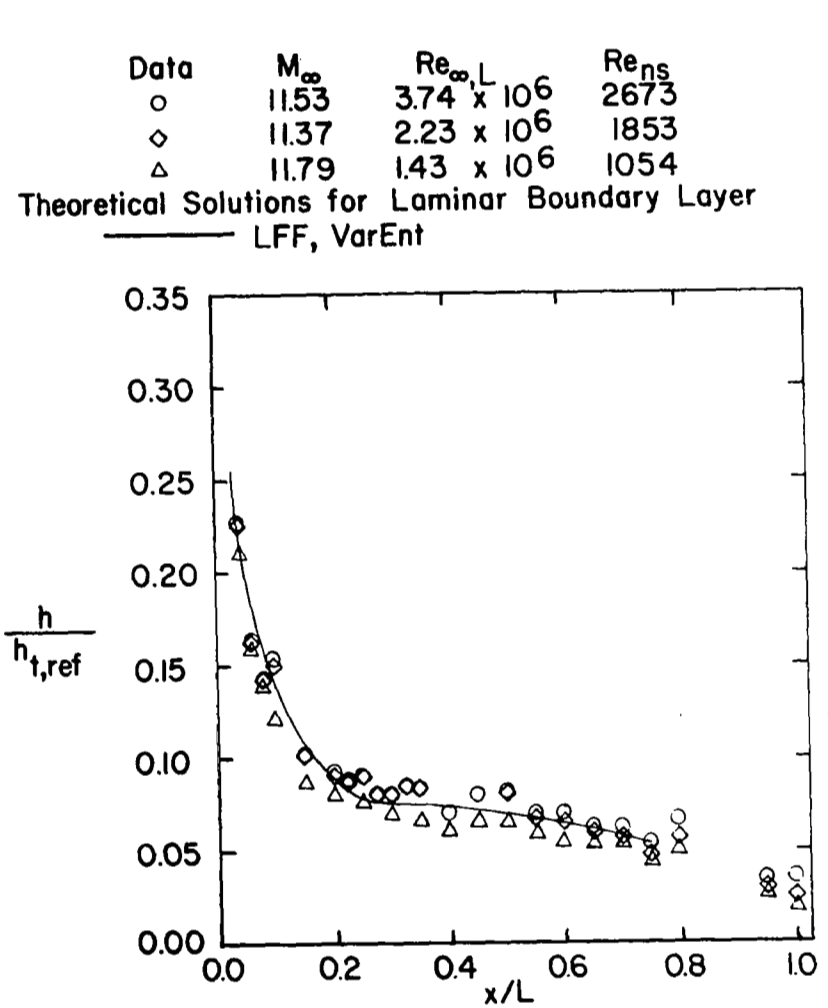

Fig. 6. - Heat-transfer distributions from the plane of symmetry of the tile-roughened model (Tunnel F) illustrating incipient transition.

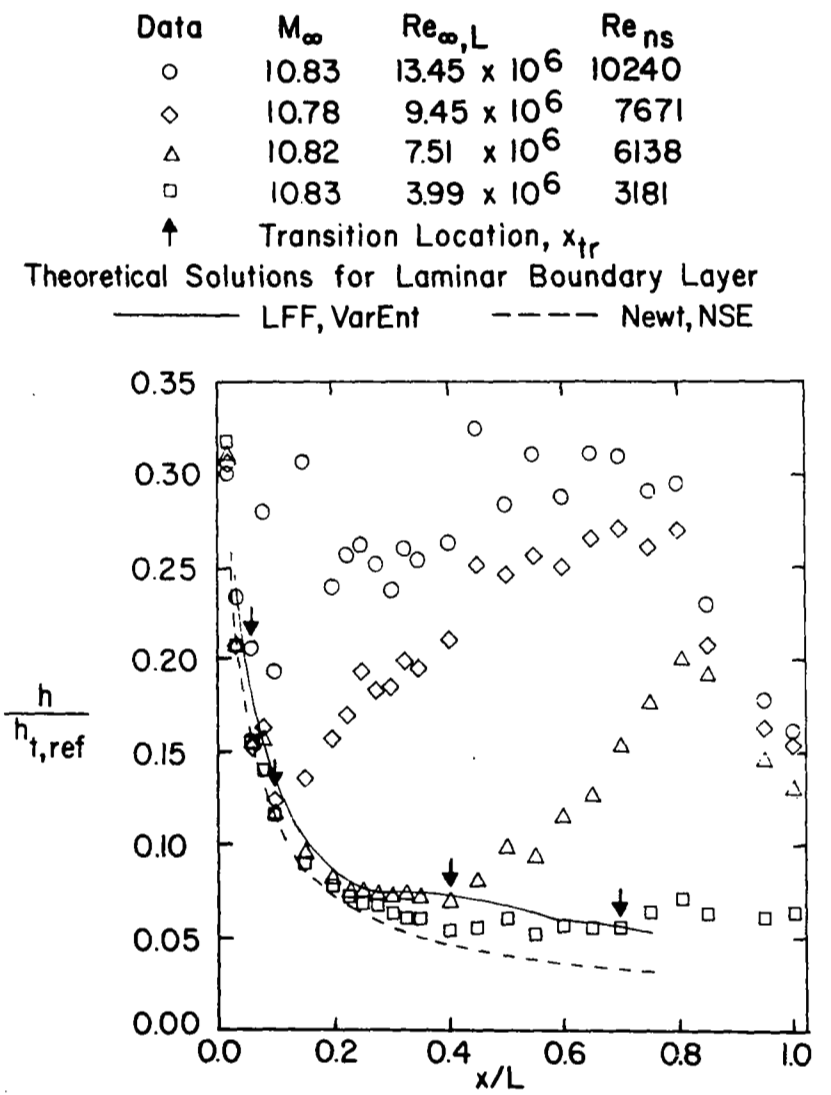

Fig. 7. - Heat-transfer distribution from the plane of symmetry of the grit-roughened model (Tunnel F) compared with theoretical laminar distributions.

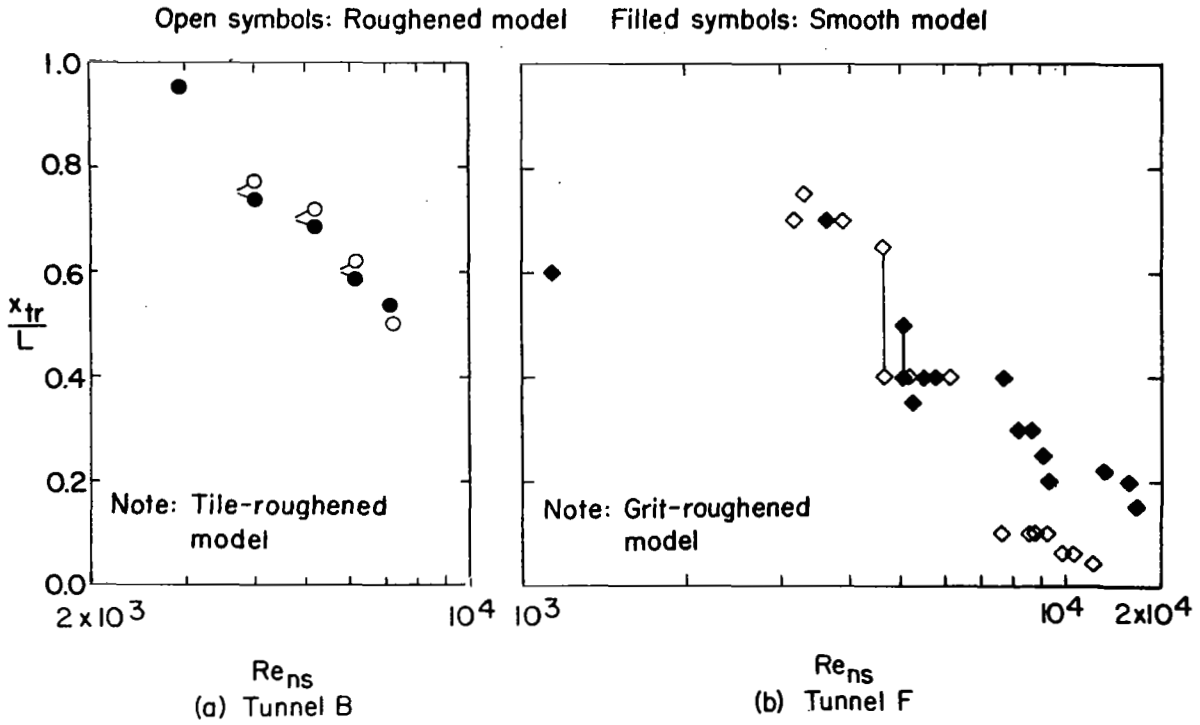

Fig. 8. - The effect of roughness on the transition locations for $\alpha = 30°$.

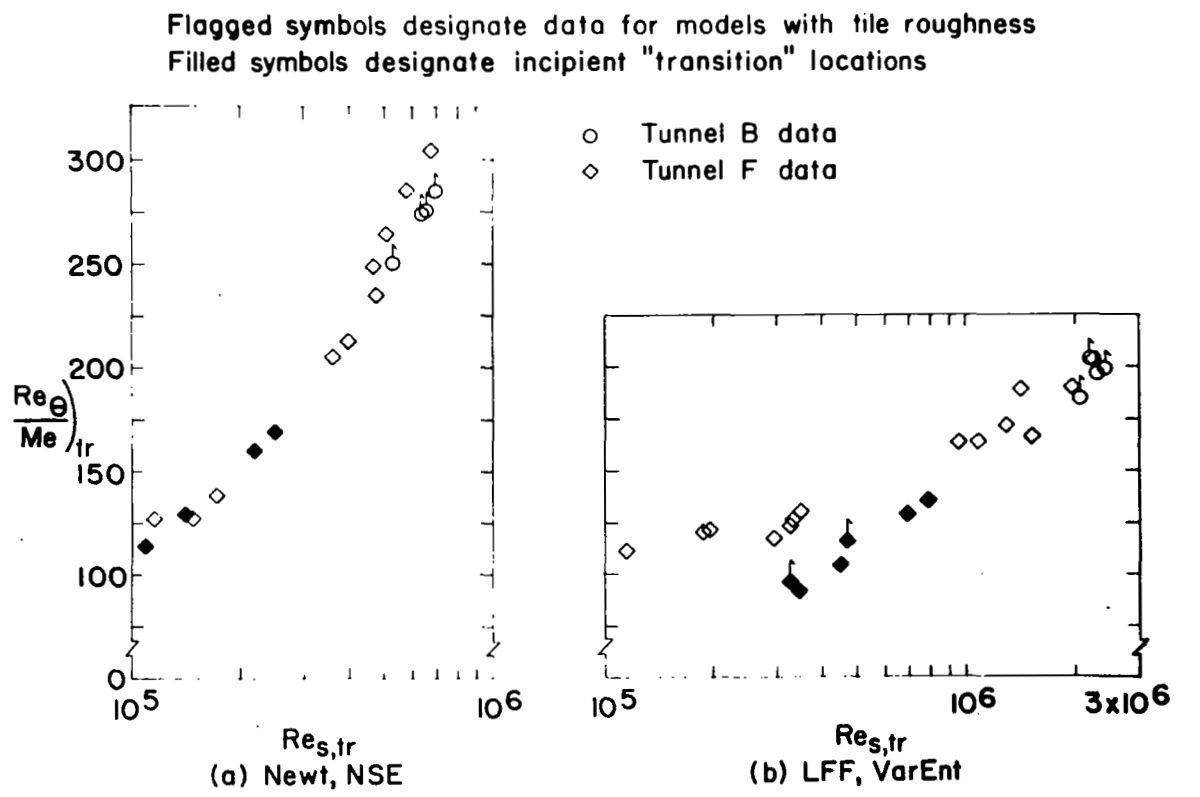

Fig. 9. - Transition correlations for the roughened Orbiter model at $\alpha = 30°$.